

Water Environment and Nanostructural Network in a Reactive Powder Concrete

A. Feylessoufi,^a F. Villiéras,^b L. J. Michot,^b P. De Donato,^b J. M. Cases^b
& P. Richard^a

^aLaboratoire des Matériaux, Groupe Bouygues, Direction Scientifique, Challenger, 1 avenue Eugène Freyssinet, 78 061 Saint Quentin en Yvelines France

^bLaboratoire Environnement et Minéralurgie, ENSG et URA 235 CNRS, rue du Doyen Marcel Roubault, BP 40, 54 501 Vandoeuvre les Nancy France

(Received 14 April 1995; accepted 10 July 1995)

Abstract

A Reactive Powder Concrete (RPC) with an average compressive strength of 230 MPa was studied by diffuse reflectance infrared Fourier transformed spectroscopy (DRIFTS), controlled rate thermal analysis (CRTA) and low temperature nitrogen adsorption–desorption volumetry. Different water environments are observed by DRIFTS. The CRTA experiments coupled to mass spectrometric analyses allow us to differentiate various gases corresponding to adsorbed molecules and to the pyrolysis of different species. In particular the organic species added during processing can be observed. Adsorption experiments reveal a low specific surface area showing an intimate reaction between the starting components during processing. Furthermore, they show that the RPC can be considered as an open network of pores of various diameters.

Key words: Concrete, ultra high performance, mesoporosity, nanostructure, network, water status, spectrometric analysis, thermal analysis, adsorption–desorption volumetry.

INTRODUCTION

In civil engineering, the development of concrete is linked to its mechanical performance.¹ Therefore, intensive research efforts have been devoted to the improvement of the mechanical properties of concretes. One of the first breakthroughs was the invention of High

Performance Concrete (HPC) characterized by a compressive strength of 100–120 MPa and high level durabilities which lead to interesting realizations in civil engineering.

Concrete research has demonstrated the influence of elaboration processes for obtaining higher performances. In particular, the importance of physical and chemical mechanisms in the densification and phase development was revealed as concretes exhibiting high compressive strength, up to 650 MPa, can be obtained with compact samples, hot cured under pressure in hydrothermal conditions.² Other improvements have been obtained by adding polymer components to MDF concretes³ or by controlling the proportions and the mechanical behaviour of components in the case of DSP concretes.⁴ In spite of these performances, the use of these ultra high strength concretes as building materials was impaired due to their manufacturing behaviour, their insufficient durability and their low strength or fragility in tensile tests. Therefore, applications have been limited to some specific aims such as flooring and nuclear waste storage.

Recently, a new family of ultra high strength concretes named reactive powder concretes (RPC) has been elaborated.⁵ The compressive strength of these materials ranges from 200 up to 800 MPa; ductility is important, break-down energies range between 1200 and 40 000 J/m² and ultimate tensile strain before fracture is 7×10^{-3} . Such ultra high strength materials can normally be used for building purposes. For instance, the test of a 10 m RPC pretensioned

beam without conventional reinforcing has been successful⁶ showing the potentialities of RPC in civil engineering. The development of these materials could lead to drastic modifications in the design and structural analysis of future construction projects.

It has been shown⁷ that the high mechanical and physical performances of RPC were partly due to the reduction of porosity as measured by mercury porosimetry. This suggests different mechanisms of capillary exchanges and status of water. Investigation methods must therefore be adapted in order to determine the shape, scale and connectivity of the porosity, i.e. the water content and its mobility. In this paper, a RPC having a compressive strength of 230 MPa has been studied using diffuse reflectance infrared Fourier transformed spectroscopy (DRIFTS), controlled rate thermal analysis (CRTA) and nitrogen adsorption-desorption volumetry at 77K.

MATERIAL AND METHODS

Material

The RPC used in this study was elaborated using the following components:

component	mass ratio
Type V — portland cement	1
fine sand (150–400 μm , > 99% quartz)	1.1
Undensified silica fume (18 m^2/g)	0.25
Polymelamine sulfonate superplasticizer	0.044
Water	0.15

The concrete was mixed, cast and vibrated as a conventional concrete. Elaborated samples are 70 mm in diameter and 140 mm long. They were cured in water at 20°C for 7 days, in water at 90°C for 4 days and then dried in air at 90°C for 2 days. The cure process is performed to stabilize the mechanical and physical properties of the specimen. After their curing process, the samples have a density of $2.47 \times 10^6 \text{ g/m}^3$.

Mechanical tests, carried out with the cylindrical pieces, yielded the following results: average compressive strength 230 MPa (Perrier machine); dynamic Young modulus 59 GPa and Poisson ratio 0.16 (Grindosonic machine).

Physical analyses were performed on samples taken from the core of the cylindrical pieces. Samples were dry ground in an agate mortar or used as millimeter particles.

METHODS

Infrared spectroscopy

Diffuse reflectance spectra were recorded on a FTIR spectrometer (Bruker IFS88) associated to a diffuse reflectance attachment (Harrick Corporation). The analyses were made on 0.07 g of powdered solid diluted in 0.37 g of a non absorbing matrix of KBr, used as reference. This technique enhances the bands of weak intensities and, in particular, the bands corresponding to surface species.^{8,9}

Controlled rate thermal analysis

In the CRTA method, the heating rate of the sample is not constant but controlled by the sample as the rate of desorbed gas is kept constant (or controlled) over the entire temperature range of the experiment.^{10–12} This system operates in the reverse way of conventional thermal analysis because the measured temperatures are dependent on the properties of the sample. The rate of desorption, or gas flow evolved from the sample, is controlled by keeping constant the pressure drop through a restriction leading to high dynamic vacuum. The gases are then analyzed by mass spectrometry (Balzers QMG 420 C).

For a constant rate of water vapor loss, the temperature vs time data may be immediately converted into temperature vs mass loss data if the total weight loss is measured at the end of the experiment. Experiments were carried out on powder and millimeter particles using 0.3 g of sample and a residual pressure of 2 Pa.

Nitrogen adsorption-desorption

Nitrogen adsorption-desorption isotherms were carried out at 77K on classical step by step volumetric equipment. 20 g of powder were outgassed under a residual pressure of 0.1 Pa for 20 h at 200°C. The specific surface areas were determined using BET treatment,¹³ the presence of micropores was assessed by using the t-plot method¹⁴ and the mesopore distribu-

tion (size 2–45 nm) was determined using a parallel pore model proposed by Delon and Dellyes¹⁵ for the case of phyllosilicates.

RESULTS

Infrared spectroscopy

The spectrum obtained on the powder is displayed Fig. 1. Three regions appear:

3800–2400 cm^{-1} range. This is the domain of OH stretching vibrations of water molecules and structural or superficial hydroxyl groups. The wide band centered at 3346 cm^{-1} results from the combination of at least two kinds of molecular water: (i) physisorbed water that

can result in the broad band centered at 3400 cm^{-1} , and (ii) more structured water at 3345 cm^{-1} , probably trapped in the porosity. Two OH stretching bands are superimposed to water stretching bands: a sharp band at 3643 cm^{-1} and a shoulder at 3694 cm^{-1} .

2200–1300 cm^{-1} range. This domain corresponds to combinations and overtones of bands for the 1300–600 cm^{-1} region and to deformation vibrations of different kinds of water molecules. Most of these bands arise from combinations and overtones of bands of quartz (2240, 1982, 1871, 1795, 1678, 1604 and 1490 cm^{-1}). The region of deformation vibrations of water molecules (1640 to 1610 cm^{-1}) cannot be assigned unambiguously as combination and overtone bands superimpose

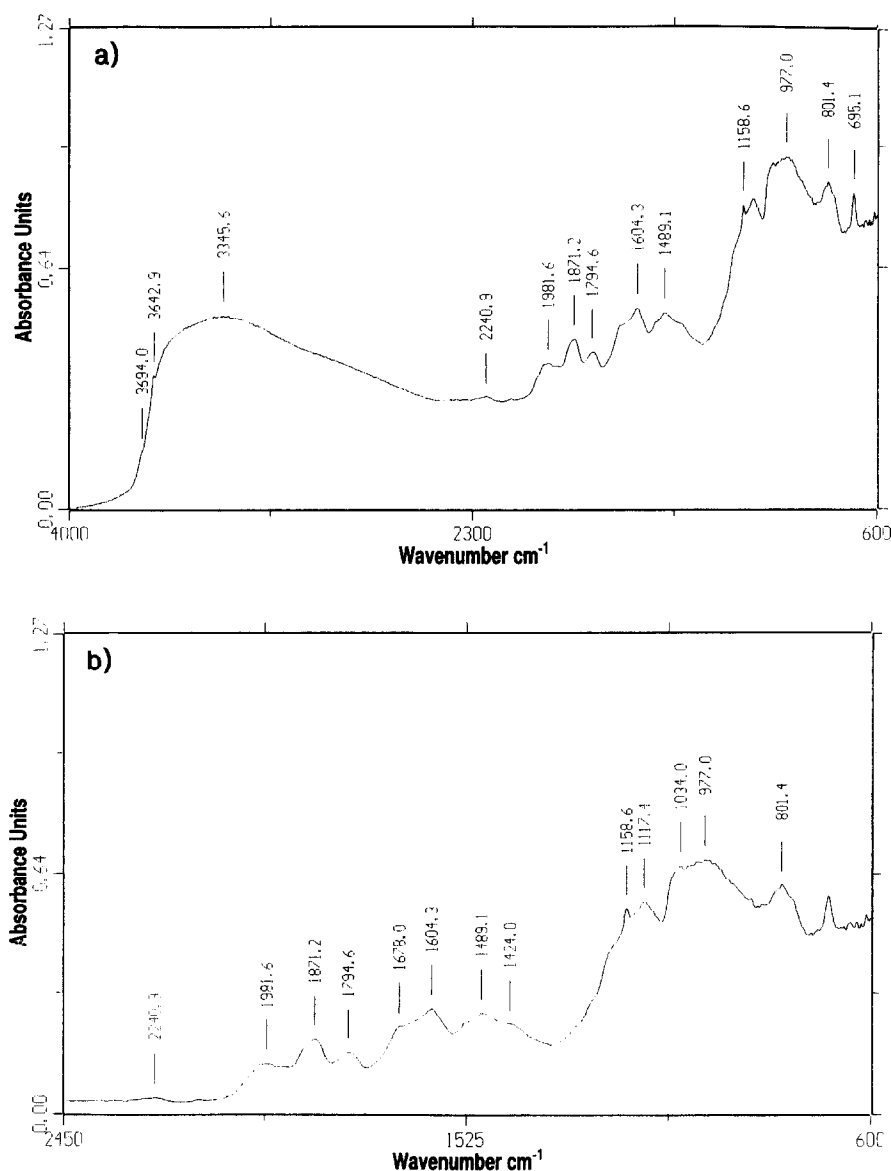


Fig. 1. (a) Diffuse reflectance infrared spectrum of powdered RPC. (b) Magnification of the 2450–600 cm^{-1} region.

in this region. However, a shoulder appears around 1630 cm^{-1} .

$1300\text{--}600\text{ cm}^{-1}$ range. This region corresponds to stretching vibrations of Si–O and S–O groups. The 1159 , 1034 , 977 , 801 and 695 cm^{-1} bands can be assigned to quartz whereas the 1117 cm^{-1} band can be assigned to S–O vibration, probably in a sulfate compound.

Controlled rate thermal analysis

Figure 2 displays the thermal analysis obtained on millimeter particles and on powder. It shows that outgassing is shifted by about 60°C toward higher temperatures when millimeter particles are used indicating diffusion phenomena. On both samples, a small slope change is observed around 250°C due to the desorption of a new

family of gas. Above this temperature, outgassing curves are superimposed showing that the diffusion barrier is overcome. Mass spectra obtained in the case of the powdered sample are displayed in Fig. 3.

Water loss ($m/z=18$) ends around 600°C . The detailed analysis of water loss (Fig. 4) shows that the break observed on Fig. 2 can be assigned to the desorption of an additional family of water. However, it is not possible to distinguish between adsorbed water (porosity) and structural water (hydroxyls).

A set of masses ($m/z=2$, 12 , 66 , 78 and 92) is observed between 300 and 600°C . It corresponds to organic species of high molecular mass and can be assigned to desorption of the superplasticizer trapped in the porosity or adsorbed on RPC surface.

The release of carbon dioxide ($m/z=12$, 28 and 44) starts at 400°C with a maximum centered at 800°C . Its evolution is plurimodal. The decomposition of sulfates ($m/z=32$, 48 , 64 , and 66) starts at 600°C . Their evolutions are plurimodal too, with maxima centered around 780 and 950°C and are partly superimposed with carbon dioxide.

The evolution of hydrogen ($m/z=2$) is not clearly understood.

Nitrogen adsorption–desorption

The adsorption–desorption isotherm obtained on the powdered sample outgassed at 200°C is displayed in Fig. 5(a). It features an important desorption hysteresis typical of a mesoporous

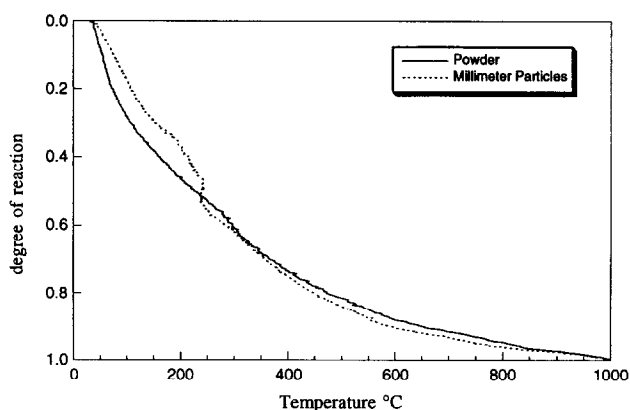


Fig. 2. Controlled Rate Thermal Analysis of powdered and millimetric particles of RPC.

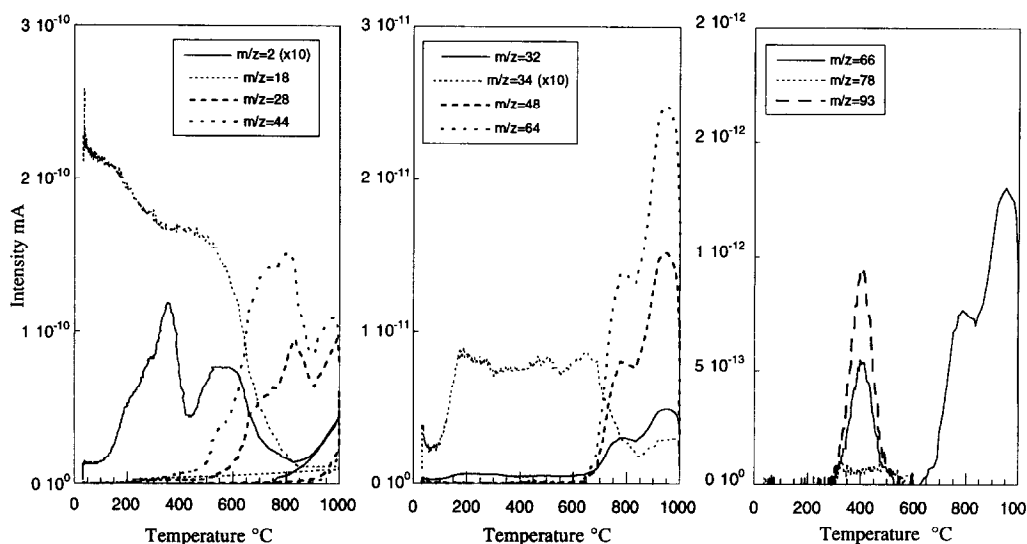


Fig. 3. Evolution of the gases released from powdered RPC during the CRTA experiment.

sample (Type IV isotherm). The specific surface area derived from the BET treatment is $0.93 \pm 0.1 \text{ m}^2 \cdot \text{g}^{-1}$ and the energetic constant, $C=105$, is a classical value for nitrogen adsorption. The t-plot method (Fig. 5(b)) indicates the presence of some microporosity (diameter lower than 2 nm). The equivalent surface area due to micropores derived from the intercept at the origin is equal to $0.2 \pm 0.1 \text{ m}^2 \cdot \text{g}^{-1}$ and the non microporous surface area derived from the slope is equal to $0.75 \pm 0.1 \text{ m}^2 \cdot \text{g}^{-1}$. From $P/P_0=0.9$, the t-plot curve deviates to high adsorption quantities due to adsorption in mesopores (2 to 45 nm) generated by inter-particle voids.

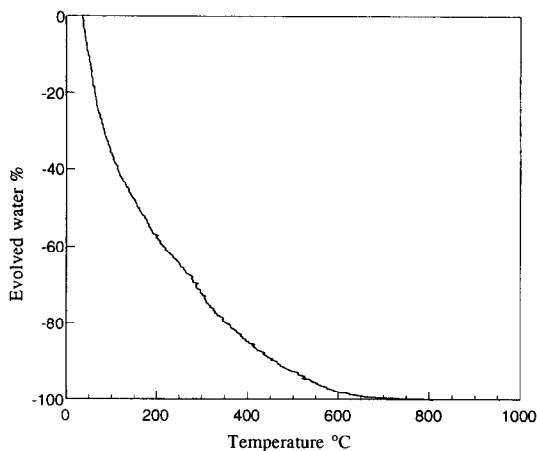


Fig. 4. Integrated water loss from powdered RPC derived from mass spectrometric analysis.

The repartition of mesopores volumes was calculated from desorption isotherm considering cylindrical and slit shaped mesopores. The second model gives the most reliable results which are presented in Fig. 6. Mesopore repartition displayed 4 families: mesopores greater than 15 nm, centered at 9, 5 and 2.6 nm.

The specific surface area of the concrete can then be broken down in the following way:

$0.2 \text{ m}^2 \cdot \text{g}^{-1}$ of micropores corresponding to a geometric volume of 0.07 mm^3 .

$0.40 \text{ m}^2 \cdot \text{g}^{-1}$ of mesopores centered at 2.6 nm corresponding to a geometric volume of 0.52 mm^3 .

$0.22 \text{ m}^2 \cdot \text{g}^{-1}$ of mesopores centered at 5 nm corresponding to a geometric volume of 0.48 mm^3 .

$0.11 \text{ m}^2 \cdot \text{g}^{-1}$ of mesopores centered at 9 nm corresponding to a geometric volume of 0.55 mm^3 .

$0.11 \text{ m}^2 \cdot \text{g}^{-1}$ of mesopores greater than 15 nm which can be assigned to external surface area corresponding to a geometric volume of 1 mm^3 .

The amount of water trapped in this porosity ($<40 \text{ nm}$) corresponds to $2.6 \text{ mg} \cdot \text{g}^{-1}$. This represents approximately 10% of the total water loss before 200°C measured by CRTA revealing an important macroporosity that cannot be probed by gas adsorption techniques.

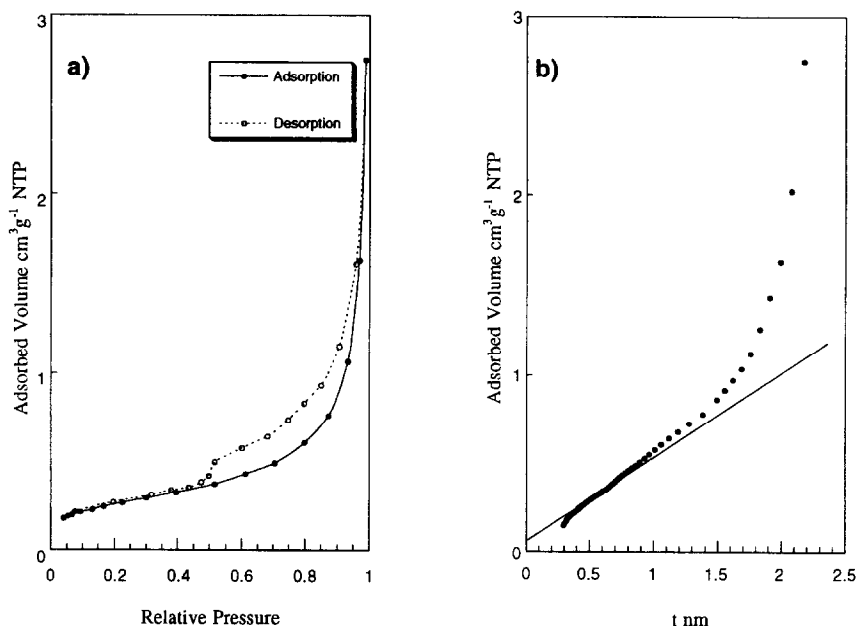


Fig. 5. (a) Adsorption-desorption isotherm of nitrogen at 77K on powdered RPC outgassed at 200°C under a residual pressure of 0.1 Pa. (b) t-Plot derived from the adsorption isotherm of (a).

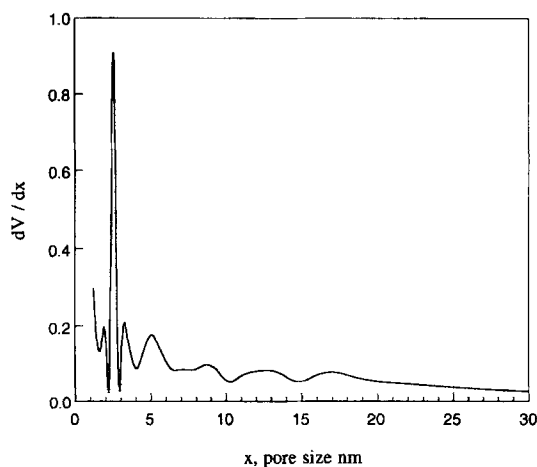


Fig. 6. Mesopore size distribution of powdered RPC.

DISCUSSION

The present study shows that reliable results can be obtained about the structural and textural properties of RPC concretes from a combination of spectroscopic and physico-chemical methods. Three main results have been obtained:

Infrared spectroscopy definitely shows that the powdered concrete contains adsorbed water. Furthermore, two families of water could be distinguished. CRTA coupled to mass spectrometry shows that water is the main gas contained in the studied concrete. However, due to diffusion phenomena and superimposition of structural evolved water, this method does not give information on the different adsorption sites of water. This information is obtained by nitrogen adsorption-desorption which allows us to distinguish between several classes of porosity ranging from 0 to 50 nm. The different pores are connected to each other and water can diffuse out of the particles. This is confirmed by the CRTA obtained on millimeter particles. It can then be concluded that RPCs are made of an open network of pores.

The polymer added in the formulation is not observed by infrared spectroscopy as the stretching carbonyl vibration is not observed. In the case of a sample with specific surface area of $1 \text{ m}^2 \cdot \text{g}^{-1}$, the diffuse reflectance method appears to be sensitive to adsorbed organic molecules if the surface coverage is around one. In our case, one can conclude that less than one layer of polymer is adsorbed on the surface of RPC. However, the

CRTA coupled to mass spectrometry is sensitive enough to detect the desorption of the polymer. One can note that some water molecules can be associated with the superplasticizer which is a very hydrophilic molecule.

The total specific surface area ($0.93 \text{ m}^2 \cdot \text{g}^{-1}$) is lower than the surface of the undensified silica fume used in the formulation. Indeed, the initial surface area of the concrete would be around $1.9 \text{ m}^2 \cdot \text{g}^{-1}$ if the added water is not taken into account and the surface of the other component considered as negligible. The fact that the final surface area is lower clearly shows that the silica fume has reacted with the other components of the concrete to form compact and solid agglomerates.

CONCLUSIONS

The study of a RPC by infrared spectroscopy, controlled rate thermal analyses coupled to mass spectrometry and adsorption-desorption volumetry shows that this concrete displays an open network of micro and mesopores. This porosity is filled by molecular water which can diffuse out of the solid.

REFERENCES

1. Freyssinet, E., High-early-strength concrete with Portland cement. *Cement and Cement Manufacture*, **9** (1936) 71–77.
2. Roy, D. M. & Gouda, G. R., High strength generation in cement pastes. *Cement and Concrete Research*, **3** (1973) 807–820.
3. Russel, P. P., Shunkwiller, L., Berg, M. & Young, J. F., Moisture resistance of macro-defect-free cement. *Advances in Cementitious Materials — Ceramic Transactions*, **16** (1991) 501–519.
4. Bache, H. H., Densified cement ultrafine based materials, *2nd Int. Conf. Superplasticizers in Concrete*, Ottawa, June 10–12, 1981.
5. Richard, P. & Cheyrezy, M., Reactive Powder Concretes with High Ductility and 200–800 MPa Compression Strength, ACI Spring Convention, San Francisco, 1994.
6. Richard, P., Cheyrezy, M. & Dugat, L., Poutre précontrainte sans armatures passives (Pretensioned beam without conventional reinforcing), Contribution française au XII congrès de la FIP, Washington, DC, 1994.
7. Cheyrezy, M., Maret, V. & Frouin, L., Microstructural Analysis of Reactive Powder Concretes, *Cement and Concrete Research*, **25** (1995) 1491–1500.
8. Griffiths, P. R. & Haseth, J. S., *Fourier Transformed Infrared Spectroscopy*. Wiley-Interscience, New York, 1986.

9. De Donato, P., Mustin, C., Benoit, R. & Erre, R., Spatial distribution of iron and sulfur species on the surface of pyrite. *Applied Surface Science*, **68** (1993) 81–93.
10. Rouquerol, J., L'analyse thermique à vitesse de transformation constante. *Journal of Thermal Analysis*, **2** (1970) 123–140.
11. Rouquerol, J., Controlled transformation rate thermal analysis: the hidden face of thermal analysis. *Thermochimica Acta*, **144** (1989) 209–224.
12. Rouquerol, J., Bordère, S. & Rouquerol, F., Controlled rate thermal evolved gas analysis: recent experimental set-up and typical results. *Thermochimica Acta*, **203** (1992) 193–202.
13. Brunauer, S., Emmett, P. H. & Teller, E., Adsorption of gases in multimolecular layers. *J. Amer. Soc.*, **60** (1938) 309.
14. De Boer, J. H., Lippens, B. C., Linsen, B. G., Broekoff, J. C. P., Van Den Heuvel, A. & Osinga, Th., The t-curve of multimolecular N₂ adsorption. *Journal of Colloid Interface Science*, **21** (1966) 405–414.
15. Delon, J. F. & Dellyes, R., Calcul du spectre de porosité des minéraux phylliteux. *C. R. Acad. Sci. Paris, Série D*, **265** (1967) 1161–64.